***Supplementary Material***

# AFM resolves effects of ethambutol on nanomechanics and nanostructures of single dividing mycobacteria in real-time

**Yangzhe Wu †, Ronald C. Sims, Anhong Zhou ***

Department of Biological Engineering, 4105 Old Main Hill, Utah State University, Logan, Utah 84322-4105, U.S.A. Email: Anhong.Zhou@usu.edu

† Current address: Department of Microbiology and Immunology, College of Medicine, University of Illinois at Chicago, Chicago, IL 60612 USA.

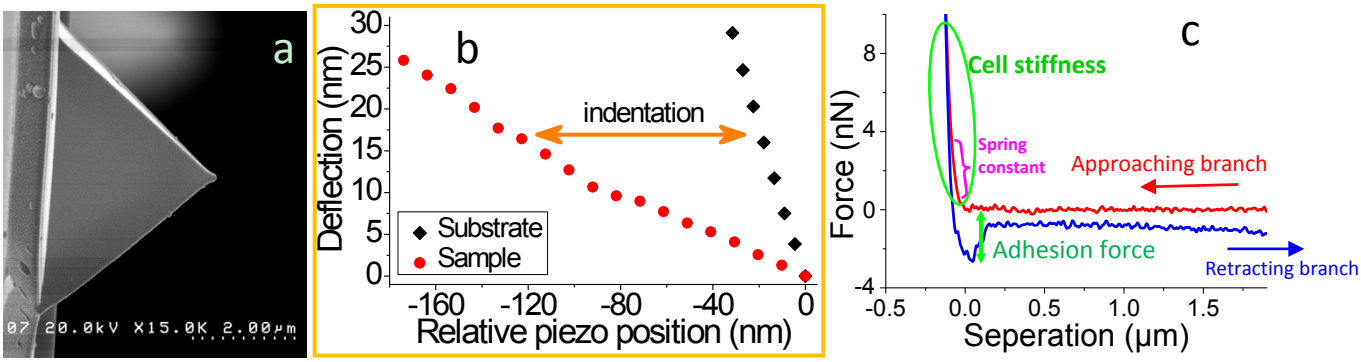


**Figure S1. (a)** Scanning electron microscope (SEM) image of silicon nitride probe tip coated with 10 nm of gold before imaging. SEM shows the tip with a pyramidal shape, 36(degree) tip half-angle, and 3.2 µm tip length. **(b)** An example of cell indentation determination. Deflection of the cantilever vs. piezo movement for the interaction of a silicon nitride tip with hard substrate and sample surface shows the relationship between the indentation depth of a cell sample and deflection of the probe cantilever. **(c)** An example of force curve, showing both approaching and retracting branches. The part of approach branch highlighted with green oval curve was used to determine Young's modulus that was conducted using software SPIP, and the part of retracting branch highlighted with green double-arrow was used to determine adhesion force. For spring constant determination, the part of approaching branch highlighting with pink Right Brace was used to perform calculation.

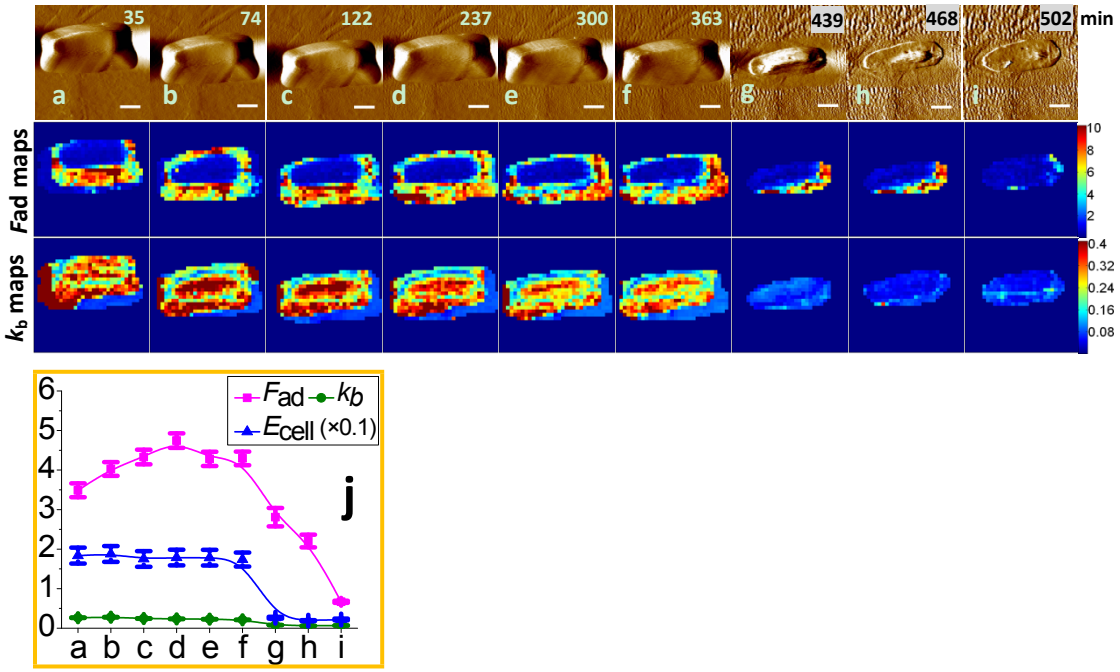


**Figure S2.** Consecutive measurements of nanomechanical dynamic alterations of EMB (25 μg/ml) treated *M. JLS*, which were acquired using contact mode AFM in culture media (without fixation). The serial images of EMB induced cell wall destruction of *M. JLS* are shown in the first row **(a-i)**, and the maps of adhesion force (nN) and spring constant (N/m) acquired at each time point are correspondingly displayed in the second and the third rows, respectively. Graph **(j)** shows statistical analyses of adhesion force ($F_{ad}$, nN), spring constant ($k_b$, N/m), and Young's modulus ($E_{cell}$, MPa), in which letters 'a-i' of x-axis correspond to the respective image in the first row. The frames of row 1 were taken from **Flash III-2**. Scale bar: 500 nm.

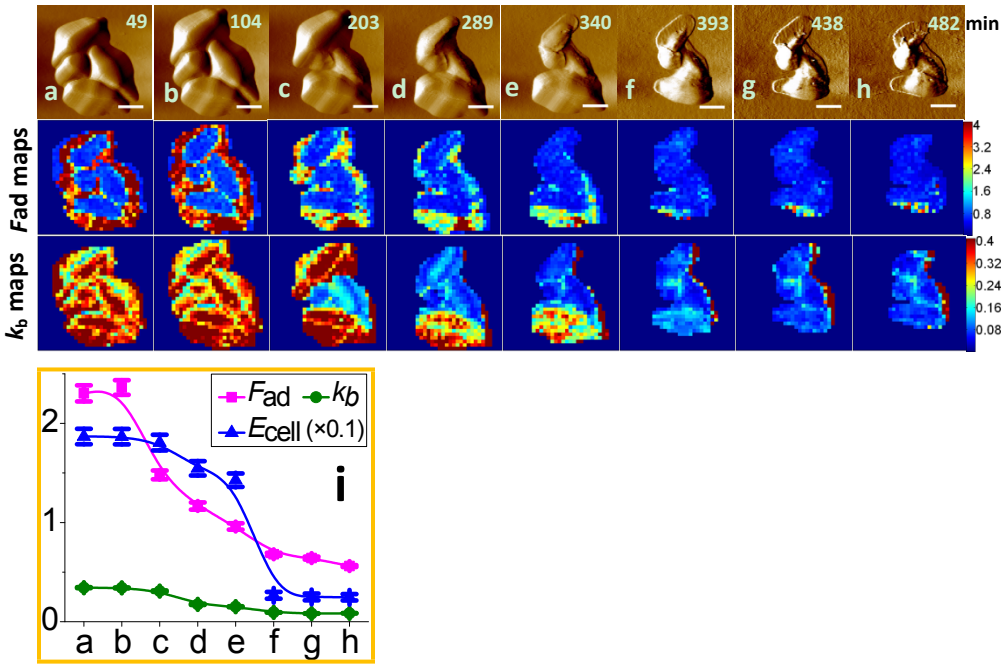


**Figure S3.** Consecutive measurements of nanomechanical dynamic alterations of EMB (50 µg/ml) treated *M. JLS*, which were acquired using contact mode AFM in culture media (without fixation). The serial images of EMB induced cell wall destruction of *M. JLS* are shown in the first row **(a-h)**, and the maps of adhesion force (nN) and spring constant (N/m) of cells acquired at each time point are correspondingly displayed in the second and the third rows, respectively. Graph **(i)** shows statistical analyses of adhesion force ($F_{ad}$, nN), spring constant ($k_b$, N/m), and Young's modulus ($E_{cell}$, MPa), in which letters 'a-h' of x-axis correspond to the respective image in the first row. The frames of row 1 were taken from **Flash IV-1**. Scale bar: 800 nm.

# Flash files:

- **Flashes I-1**, **I-2**:

  Contact mode images of dividing *M.JLS* without any treatments;

  All division phases can be clearly seen;

- **Flash I-3:**

  AC mode images of dividing *M.JLS* without any treatments;

  Division phases A-E can be clearly seen;

- **Flashes II-1, II-2:**

  Contact mode images of 10 μg/ml EMB treated dividing *M.JLS*;
  The division phase of cell in Flash II-1 might be at C or D;
  The division phase of cell in Flash II-2 might be at A or B;

- **Flashes III-1, III-2:**

  Contact mode images of 25 μg/ml EMB treated dividing *M.JLS*;
  The division phase of cell '5' in Flash III-1 might be at E;
  The division phase of cell in Flash III-2 might be at A or B;

- **Flashes IV-1, IV-2:**

  Contact mode images of 50 μg/ml EMB treated dividing *M.JLS*;
  The division phase of cells in Flashes IV-1 and IV-2 might be at A or B, or even phase C because high concentration of EMB would exert dominant influences on cell wall collapse in this context.